



Published in final edited form as:

ACS Nano. 2013 March 26; 7(3): 2566–2572. doi:10.1021/nn305949h.

## Observations of Carbon Nanotube Oxidation in an Aberration-Corrected, Environmental Transmission Electron Microscope

Ai Leen Koh<sup>§,\*</sup>, Emily Gidcumb<sup>‡</sup>, Otto Zhou<sup>‡,†</sup>, and Robert Sinclair<sup>§,†,\*</sup>

<sup>§</sup>Stanford Nanocharacterization Laboratory, Stanford University, Stanford, California 94305, USA

<sup>‡</sup>Curriculum in Applied Sciences and Engineering, University of North Carolina at Chapel Hill, Chapel Hill, North Carolina 27599, USA

<sup>†</sup>Department of Physics and Astronomy, University of North Carolina at Chapel Hill, Chapel Hill, North Carolina 27599, USA

<sup>‡</sup>Department of Materials Science and Engineering, Stanford University, Stanford, California 94305, USA

### Abstract

We report the first direct study on the oxidation of carbon nanotubes at the resolution of an aberration-corrected environmental transmission electron microscope (ETEM), as we locate and identify changes in the same nanotubes as they undergo oxidation at increasing temperatures *in-situ* in the ETEM. Contrary to earlier reports that CNT oxidation initiates at the end of the tube and proceeds along its length, our findings show that only the outside graphene layer is being removed and on occasion, the interior inner wall is oxidized, presumably due to oxygen infiltrating into the hollow nanotube through an open end or breaks in the tube. We believe that this work provides the foundation for much scientific understanding of the mechanism underlying the nanotube oxidation process, as well as guidelines to manipulate their structure or prevent their oxidation.

### Keywords

Carbon nanotubes; oxidation; environmental TEM; aberration-corrected TEM

Because of our natural environment, oxidation of matter has fundamental importance. For instance, under controlled conditions, the oxidation of silicon produces sub-2 nm gate oxides for field effect transistors. In an uncontrolled fashion, the oxidation of metals and alloys results in countless corrosion problems. Since their discovery in 1991 carbon nanotubes (CNTs)<sup>1</sup> have found an increasing number of applications, most notably as field emission electron sources<sup>2, 3</sup> in displays<sup>4, 5</sup> or in X-ray tubes<sup>6, 7</sup> for medical applications.<sup>8, 9</sup> Carbon nanotubes have lower emission threshold fields compared to other emitter materials.<sup>10–13</sup> This, combined with their excellent structural integrity, high electrical and thermal conductivity and their relatively inexpensive fabrication costs, makes them ideal candidates as electron field emitters.

In a laboratory setting, field emission measurements of CNTs are usually carried out using an ultrahigh vacuum system with base pressure of  $\sim 10^{-7}$  mbar or better.<sup>14, 15</sup> Under less stringent vacuum conditions, carbon nanotubes are found to exhibit lower emission currents and reduced lifetimes.<sup>15, 16</sup> It has been hypothesized that field emission of CNTs under less

\*Corresponding Authors: Ai Leen Koh: alkoh@stanford.edu; Robert Sinclair: bobsinc@stanford.edu.

ideal vacuum conditions leads to the destruction of smaller diameter nanotubes through ion bombardment or arcing.<sup>16</sup> Dean and coworkers<sup>15</sup> found that the emission currents of single-walled CNTs decreased when they were emitting in low pressures of oxygen and water vapor, and suggested that this was due to reactive sputter etching. Shortly after the discovery of CNTs, several groups attempted to utilize the oxidation process to manipulate their structures, for instance by opening up their terminating cap, or by thinning the tubes.<sup>17, 18</sup> In the literature, these oxidation steps were usually performed in an external laboratory setting and the state of the oxidized samples was surveyed *a posteriori* with a transmission electron microscope (TEM). However, because of their nano-scale, no direct study has been performed on the underlying mechanism of their oxidation. With the recent availability of environmental gaseous cells incorporated into aberration-corrected transmission electron microscopes (TEM),<sup>19, 20</sup> this has now become possible.

In this article, we report the first direct study on the oxidation of carbon nanotubes at the high resolution of an aberration-corrected environmental TEM (ETEM), as we locate and identify changes in the same nanotubes as they undergo oxidation at increasing temperatures *in-situ* in the ETEM. The instrument used in this work is a Titan 80–300 ETEM equipped with a spherical aberration (Cs) corrector in the image-forming (objective) lens and a monochromator. The environmental chamber surrounds the specimen holder within the imaging objective lens<sup>21–23</sup> and can allow gas pressures up to about 20 mbar. As there are no membranes in the electron beam path, the basic instrumental resolution of sub-0.1 nm is maintained. We carried out our imaging experiments using 80 keV electrons, which is supposed to be below the knock-on displacement energy of carbon atoms in single wall carbon nanotubes,<sup>24</sup> and with the aberration corrector and monochromator the resolution of carbon atoms in single layer graphene, separated by 0.142 nm, is routinely achieved, as also reported previously.<sup>25</sup> All images were acquired with the Cs coefficient adjusted to approximately  $-15\mu\text{m}$  and using slightly overfocus conditions. Accordingly, the positions of the carbon atoms correspond to bright intensities in the aberration-corrected TEM images.<sup>26, 27</sup>

## RESULTS AND DISCUSSION

### TEM Characterization of as-synthesized carbon nanotubes

The CNTs investigated in this work were multi-wall carbon nanotubes fabricated by chemical vapor deposition (CVD) and arc-discharge methods, as described elsewhere,<sup>28, 29</sup> and are used for X-ray sources.<sup>8, 9, 30, 31</sup> Fig. 1 (a) and (b) show low-magnification, aberration-corrected TEM images of the CVD and arc-discharge CNTs, respectively. Representative high-magnification TEM images of the nanotubes synthesized using these processes are shown in Fig. 1(c) and (d), respectively. The CNTs are found in bundles with a layer of amorphous carbon overcoat around them. Using measurements on 50 nanotubes from each sample type, the present CVD-grown CNTs have between 1 and 6 graphitic layers with outer diameters ranging from 2 to 11 nm. The arc-discharge CNTs have between 4 and 34 walls and their outer diameters vary between 6 nm and 31 nm. The separation of the nanotube walls is equal to the graphitic basal plane spacing of 0.34 nm.

### *In-situ* high-vacuum heating of CNTs

A control set of CNT samples was transferred onto molybdenum TEM grids coated with holey carbon film and heated *in-situ* in the TEM under high vacuum conditions (about  $1.2 \times 10^{-7}$  mbar) to 300°C, 400°C and 520°C. The nanotubes were tracked and high-resolution TEM imaging was performed on the same tubes at each of these temperatures to establish any effects of heating alone. Fig. 2 shows the same nanotube during heating under high-vacuum conditions in the TEM to 300°C, 400°C and 520°C (the control sample). The

concentric graphene cylinders are seen edge-on, with their characteristic 0.34 nm spacing and there is no change in the nanotube structure. Some of the amorphous carbon naturally produced during the fabrication graphitizes, but there is no loss or change of diameter of the nanotubes.

It has been reported in the literature that the threshold for knock-on damage for carbon nanotubes can be lower than the reported 86 kV,<sup>24</sup> for single walled carbon nanotubes (SWNTs) with smaller diameters (*e.g.* 1 nm),<sup>32</sup> or if there are contaminants<sup>32</sup> or defects<sup>33</sup> in the carbon nanotubes. As the data reported for the present control experiment (and all experimental samples thereafter) are for multiwalled tubes with diameters larger than those reported for SWNTs, we expect them to be more resistant to electron beam irradiation at 80 kV compared to SWNTs. All our specimens were also heated to at least 300°C in the electron microscope prior to beam exposure. This is an effective way of removing contaminants present on CVD-grown carbonaceous material.<sup>34</sup> Indeed, our experimental findings suggest that by heating the samples under high-vacuum conditions and by carefully controlling the electron dose (see Methods and Materials section), there is no loss, damage or change in diameter of the nanotubes.

### ***In-situ* heating and oxidation of CNTs**

Oxidation studies were performed by first heating CNT samples (on different TEM grids) to 300°C in high vacuum. A few nanotubes were identified for tracking. Then, with the electron beam blanked (the reasons for this protocol, to blank the electron beam, are discussed later), 1.5mbar of research grade (99.9999% purity) oxygen was introduced into the ETEM for 15 minutes while keeping the temperature constant at 300°C. At the end of this cycle, the gas was purged from the system for 45 min while the temperature was maintained at 300°C. The microscope environmental cell vacuum pressure was measured to be about  $1.6 \times 10^{-7}$  mbar after the oxygen purge. The same nanotubes were located and imaged to identify any differences after having been exposed to oxygen. The temperature was then increased to 400°C and the oxidation process was repeated, and the same set of nanotubes was tracked and imaged at 400°C after oxygen was purged from the system. These oxidation procedures were repeated on samples mounted on different TEM grids with initial and end temperatures of 400°C and 520°C, respectively, and the electron beam was blanked when oxygen was in the environmental chamber within the ETEM. The temperatures and pressures were chosen from a combination achievable using a heating holder in the ETEM and from the known degradation of CNT emitters.<sup>14, 15</sup> Because the carbon film on the TEM grids was also oxidized during the experiments, we opted to break the three temperature set points of the control experiments (300°C, 400°C and 520°C) into two separate oxidation experiments with start and end temperatures of 300°C and 400°C, and 400°C and 520°C, respectively. This way, each grid was limited to two oxygen exposures per experiment and enough carbon film still remained on the grids to support the nanotubes for high-resolution imaging. (From our experience, even though the carbon support film also oxidizes during the experiment, it was still more stable compared to support films such as SiO<sub>2</sub> and SiN<sub>x</sub> which are not electrically conducting and charge under the electron beam).

As the synthesized nanotubes were usually found in bundles, locating the same nanotubes after heating and oxidation was not trivial. Low-magnification maps of the shapes of the holey carbon film, and the locations of the nanotubes on the film, were made so that the same nanotubes could be found. It took, on average, at least 12 hours for each experiment, including the time to heat, stabilize (from thermal drift), oxidize and locate the nanotubes. During the ETEM experiments, the oxygen pressure in the microscope chamber was monitored using a capacitance manometer (Edwards Barocell model 600) with which the microscope is equipped, and the pressure was maintained to within  $\pm 0.2$  mbar during the

oxidation process. The temperatures were kept to within  $\pm 0.1^\circ\text{C}$  during both oxidation (with the electron beam blanked) and imaging.

One important consideration during the oxidation experiment is the possible ionization of the gaseous species by the imaging electron beam. This is most easily demonstrated by the electron energy loss (EEL) spectrum with and without the gas (oxygen) present. Figs. 3(a) and (b) are EEL spectra of the low-energy loss and K-shell ionization EEL spectra of oxygen which are the product of the ionization of the oxygen gas by the electron beam. On the other hand, they also demonstrate the presence of only oxygen gas present in the cell, as these are the only peaks detected, apart from those of carbon.<sup>35</sup> Therefore, in order to investigate the effect of gaseous oxygen molecules rather than ionized species, we established a protocol whereby heating and oxidation were performed without an imaging beam, and the changes on identifiable nanotubes were documented after purging the gas from the chamber. We also performed EEL spectroscopy after the gas was purged from the microscope, to verify that there is no residual oxygen gas remaining in the system after the gas purge (black spectrum in Fig. 3(a)).

Fig. 4 shows a three-walled nanotube at  $300^\circ\text{C}$  (Fig. 3a), at  $300^\circ\text{C}$  after 1.5 mbar oxidation for 15 min (Fig. 3b), and at  $400^\circ\text{C}$  after 1.5 mbar oxidation for 15 min (Fig. 3c). Higher-magnification insets are presented in panels (d–f) respectively. It is clear that only the outside graphene cylinder is being removed. Previously it has been thought that CNT oxidation initiates at the end of the tube<sup>17, 18</sup> and proceeds along its length: these images show that this is not the case. This view is supported by observations at the ending cap of individual nanotubes, as shown in Fig. 5. Despite the expected higher energy of the atoms at the cap, it is the outer wall which is oxidized and removed first. Fig. 5b shows that after 1.5 mbar oxidation at  $300^\circ\text{C}$ , the outermost wall of the nanotube (blue arrow in 5b) starts to “peel” away, and detaches more upon further oxidation at  $400^\circ\text{C}$ , but the wall remains attached onto the nanotube cap (black arrow in 5d). Fig. 5 also shows that, on occasion, the interior inner wall is oxidized first (red arrows in Figs. 5b and 5c), presumably due to oxygen infiltrating into the hollow nanotube through an open end or breaks in the tube. The interior wall thinning is representative of several nanotubes examined (on average, one out of every five) and is reproducible in our experiments.

CNTs with a larger number of walls (greater than six) are found to be more resistant to oxidation, with all walls remaining intact during the ETEM experiments. Fig. 6(a) shows a TEM image of an arc-discharge grown nanotube with nine graphitic layers taken at  $400^\circ\text{C}$ . After successive 1.5 mbar oxidation at  $400^\circ\text{C}$  and  $520^\circ\text{C}$  (Fig. 6(b) and 6(c)), some of the amorphous carbon surrounding the nanotube is etched away but the structure of the tube remains the same.

The observations described here represent a direct study on the oxidation of CNTs at the resolution of the electron microscope, and as such they provide a foundation for future work. For instance, the effects of oxygen ionization can be established by maintaining the electron beam during observation which has the added advantage of allowing continuous *in-situ* recording. Of course, during use as field emitters, any nearby gaseous species is likely to be ionized as well.<sup>36</sup> The effects of nanotube structure can be investigated to determine whether or not the initiation of the outer graphene layer is associated with defects in their atomic structure. One interesting observation in this regard is shown in Fig. 7, where an abnormal atomic-scale darker image spot is seen in the nanotube outer wall (red arrow in Fig. 7(b)) after exposure to 1.5 mbar oxygen at  $400^\circ\text{C}$ . This appears to be the initiation site for the outer-wall oxidation which is consumed roughly equally on either side of the feature, as shown in Fig. 7(c) (the image appearance in the upper left of the pictures acts as a fiducial marker). While this finding has little statistical significance at present, it does suggest an

alternative approach for determining the influence, if any, of nanotube imperfections. The array can be studied carefully for such features, and subsequent oxidation carried out to establish whether there are any systematic trends. If this does turn out to be the case, the full array of imaging and sub-nanoscale spectroscopic procedures can be brought to bear to characterize such features prior to oxidation. Furthermore, the influences of nanotube preparation, chirality, diameter *etc.*, on the oxidation mechanism are all of practical importance and are readily accessible by the procedures described here. Likewise, the combinations of temperature and pressure on the oxidation rates can be established and used for kinetic analysis. We expect that much scientific understanding can be achieved, as well as guidelines for utilizing CNT oxidation to manipulate their structure, or to prevent oxidation which might lead to degradation of the field-emitting properties of the CNT array.

## CONCLUSIONS

The oxidation of individual multiwall nanotubes under mild oxidation conditions proceeds layer by layer, starting with the outermost wall, and not initiating at the nanotube cap. Occasional oxidation occurs from the innermost wall. Multiwall nanotubes prepared by the arc-discharge method are more resistant to oxidation than few-wall nanotubes prepared by CVD, suggesting that they are better candidates for the practical applications cited in this work.

## MATERIALS AND METHODS

### CNT Synthesis and TEM Specimen Preparation

The CNTs used in this study were synthesized by chemical vapor deposition (CVD) and arc-discharge methods.<sup>28,29</sup> 300-mesh, 30 nm-thick holey carbon molybdenum TEM grids (Pacific Grid-Tech) were used for the ETEM experiments. For TEM specimen preparation, the nanotubes were suspended in ethyl alcohol. The vials were bath sonicated for about 10 minutes, or until agglomerates broke up. Then the nanotube suspension was drop cast onto the TEM grids and wicked dry using filter paper.

### ETEM Experiments

ETEM experiments were carried out using a FEI 80–300 kV environmental TEM equipped with a Cs image corrector and a monochromator and operated at 80kV, below the knock-on displacement energy of carbon atoms in single wall carbon nanotubes.<sup>24</sup> A Gatan 652 Inconel heating holder was used to heat the samples inside the microscope. Oxygen gas of research grade 6.0 (99.9999% purity) (Praxair Inc.) was used. The Cs image corrector was adjusted to about  $-15\ \mu\text{m}$  and all images presented were acquired at slightly overfocus conditions. TEM images were taken using an Ultrascan 1000 CCD camera at binning 2 ( $1024 \times 1024$  pixels) and an exposure time of 0.4 sec per image. The average dose per unit time was  $1195\ \text{e}^-/\text{\AA}^2\text{sec}$ . We estimate, conservatively, an exposure time of 30 sec per experimental condition per nanotube, including focusing and image acquisition. This gives a total exposure time of 90 sec per nanotube for the three set points per TEM grid per study, or a cumulative electron dose of  $1.1 \times 10^5\ \text{e}^-/\text{\AA}^2$ , which was at least two orders of magnitude lower than the electron dose reported to damage single wall carbon nanotubes at 80kV and under a microscope vacuum of  $6.5 \times 10^{-8}$  mbar.<sup>37</sup>

EEL spectra were acquired in monochromated TEM imaging mode, using a Gatan Tridiem 866 EEL spectrometer with a 1 mm entrance aperture. The dispersion setting was 0.03 eV/pixel, and the energy resolution for these experiments (defined by the FWHM of the zero loss peak) was 0.21 eV.

## Acknowledgments

This work is supported by the following funding sources: National Cancer Institute grants CCNE U54CA119343 (O.Z.), R01CA134598 (O.Z.), and CCNE-T U54CA151459-02 (R.S.). The authors thank Dr. Bo Gao of Xintek for providing the raw CNT materials used in this study. Use of the facilities of the Stanford Nanocharacterization Laboratory is appreciated.

## References

1. Iijima S. Helical Microtubules of Graphitic Carbon. *Nature*. 1991; 354:56–58.
2. Rinzler AG, Hafner JH, Nikolaev P, Lou L, Kim SG, Tomimek D, Nordlander P, Colbert DT, Smalley RE. Unraveling Nanotubes: Field Emission from an Atomic Wire. *Science*. 1995; 269:1550–1553. [PubMed: 17789445]
3. de Heer WA, Châtelain A, Ugarte D. A Carbon Nanotube Field-Emission Electron Source. *Science*. 1995; 270:1179–1180.
4. Wang QH, Setlur AA, Lauerhaas JM, Dai JY, Seelig EW, Chang RPH. A Nanotube-Based Field-Emission Flat Panel Display. *Appl Phys Lett*. 1998; 72:2912–2913.
5. Choi WB, Chung DS, Kang JH, Kim HY, Jin YW, Han IT, Lee YH, Jung JE, Lee NS, Park GS, et al. Fully Sealed, High-Brightness Carbon-Nanotube Field-Emission Display. *Appl Phys Lett*. 1999; 75:3129–3131.
6. Sugie H, Tanemura M, Filip V, Iwata K, Takahashi K, Okuyama F. Carbon Nanotubes as Electron Source in an X-Ray Tube. *Appl Phys Lett*. 2001; 78:2578–2580.
7. Zhou, O.; Lu, JP. X-Ray Generating Mechanism Using Electron Field Emission Cathode. US Patent. US6553096. 2005.
8. Cao G, Burk LM, Lee YZ, Calderon-Colon X, Sultana S, Lu J, Zhou O. Prospective-gated Cardiac Micro-CT Imaging of Free-Breathing Mice using Carbon Nanotube Field Emission X-ray. *Med Phys*. 2010; 37:5306–5312. [PubMed: 21089765]
9. Qian X, Tucker A, Gidcumb E, Shan J, Yang G, Calderon-Colon X, Sultana S, Lu J, Zhou O, Spronk D, et al. High Resolution Stationary Digital Breast Tomosynthesis Using Distributed Carbon Nanotube X-ray Source Array. *Med Phys*. 2012; 39:2090–2099. [PubMed: 22482630]
10. Cheng Y, Zhou O. Electron Field Emission from Carbon Nanotubes. *C R Phys*. 2003; 4:1021–1033.
11. Zhou J, Xu NS, Deng SZ, Chen J, She JC, Wang Z-L. Large-Area Nanowire Arrays of Molybdenum Oxides: Synthesis Field Emission Properties. *Adv Mater*. 2003; 15:1835–1840.
12. Zhu W, Bower C, Kochanski GP, Jin S. Electron Field Emission from Nanostructured Diamond and Carbon Nanotubes. *Solid State Electron*. 2001; 54:921–928.
13. Chueh YL, Chou LJ, Cheng SL, He JH, Wu WW, Chen LJ. Synthesis of Taperlike Si Nanowires with Strong Field Emission. *Appl Phys Lett*. 2005; 86:133112.
14. Purcell ST, Vincent P, Journet C, Binh VT. Hot nanotubes: Stable Heating of Individual Multiwall Carbon Nanotubes to 2000 K Induced by the Field-Emission Current. *Phys Rev Lett*. 2002; 88:15502.
15. Dean KA, Chalamala BR. The Environmental Stability of Field Emission from Single-Walled Carbon Nanotubes. *Appl Phys Lett*. 1999; 75:3017–3019.
16. Bonard JM, Maier F, Stöckli T, Châtelain A, de Heer WA, Salvetat JP, Forró L. Field Emission Properties of Multiwalled Carbon Nanotubes. *Ultramicroscopy*. 1998; 73:7–15.
17. Ajayan PM, Ebbesen TW, Ichihashi T, Iijima S, Tanigaki K, Hiura H. Opening Carbon Nanotubes with Oxygen Implications for Filling. *Nature*. 1993; 362:522–525.
18. Tsang SC, Harris PJF, Green MLH. Thinning and Opening of Carbon Nanotubes by Oxidation Using Carbon Dioxide. *Nature*. 1993; 362:520–522.
19. Boyes ED, Gai PL. Environmental High Resolution Electron Microscopy and Applications to Chemical Science. *Ultramicroscopy*. 1997; 67:219–232.
20. FEI Company. Online [<http://www.fei.com>]

21. Sharma R. An Environmental Transmission Electron Microscope for *in situ* Synthesis and Characterization of Nanomaterials. *J Mater Res.* 2005; 20:1685–1707.
22. Hansen TW, Wagner JB, Dunin-Borkowski RE. Aberration Corrected and Monochromated Environmental Transmission Electron Microscopy: Challenges and Prospects for Materials Science. *Mat Sci Tech.* 2010; 26:1338–1344.
23. Jinschek JR, Helveg S. Image Resolution and Sensitivity in an Environmental Transmission Electron Microscope. *Micron.* 2012; 43:1156–1168. [PubMed: 22560892]
24. Smith BW, Luzzi DE. Electron Irradiation Effects in Single Wall Carbon Nanotubes. *J Appl Phys.* 2001; 90:3509–3515.
25. Jinschek JR, Yucelen E, Calderon HA, Freitag B. Quantitative Atomic 3-D Imaging of Single/ Double Sheet Graphene Structure. *Carbon.* 2011; 49:556–562.
26. Jia CL, Lentzen M, Urban K. Atomic-Resolution Imaging of Oxygen in Perovskite Ceramics. *Science.* 2003; 299:870–873. [PubMed: 12574624]
27. Jia CL, Lentzen M, Urban K. High-Resolution Transmission Electron Microscopy Using Negative Spherical Aberration. *Microsc Microanal.* 2002; 10:174–184. [PubMed: 15306044]
28. Qian C, Qi H, Gao B, Cheng Y, Qiu Q, Qin LC, Zhou O, Liu J. Fabrication of Small Diameter Few-Walled Carbon Nanotubes with Enhanced Field Emission Property. *J Nanosci Nanotechnol.* 2006; 6:1346–1349.
29. Ebbesen TW, Ajayan PM. Large Scale Synthesis of Carbon Nanotubes. *Nature.* 1992; 358:220–222.
30. Calderon-Colon X, Geng H, Gao B, An L, Cao G, Zhou O. A Carbon Nanotube Field Emission Cathode with High Current Density and Long-Term Stability. *Nanotechnology.* 2009; 20:325707. [PubMed: 19620758]
31. Calderon-Colon, X.; Zhou, O. Carbon Nanotube-Based Field Emission X-ray Technology. In: Saito, Y., editor. *Carbon Nanotube and Related Field Emitters: Fundamentals and Applications.* Wiley-VCH Verlag GmbH & Co. KGaA; Weinheim: 2010. p. 417-436.
32. Warner JH, Schäffel S, Zhong G, Rummeli MH, Büchner B, Robertson J, Briggs GAD. Investigating the Diameter-Dependent Stability of Single-Walled Carbon Nanotubes. *ACS Nano.* 2009; 3:1557–1563. [PubMed: 19462964]
33. Crespi VH, Chopra NG, Cohen ML, Zettl A, Louie SG. Anisotropic Electron-Beam Damage and the Collapse of Carbon Nanotubes. *Phys Rev B.* 1996; 54:5927593.
34. Radosav SP, Meyer JC, Kaiser U, Stahlberg H. The Application of Graphene as a Sample Support in Transmission Electron Microscopy. *Solid State Comm.* 2012; 152:1375–1382.
35. Crozier PA, Chenna S. *In Situ* Analysis of Gas Composition by Electron Energy-Loss Spectroscopy for Environmental Transmission Electron Microscopy. *Ultramicroscopy.* 2011; 111:177–185. [PubMed: 21333854]
36. Bonard JM, Salvétat JP, Stöckli T, de Heer WA, Forró L, Châtelain A. Field Emission from Single-Wall Carbon Nanotube Films. *Appl Phys Lett.* 1998; 73:918–920.
37. Kotakoski J, Arenal R, Kurasch S, Jiang H, Skakalova V, Stephan O, Krasheninnikov AV, Kauppinen EI, Kaiser U, Meyer JC, et al. Atomistic Description of Electron Beam Damage in Nitrogen-Doped Graphene and Single-Walled Carbon Nanotubes. *ACS Nano.* 2012; 6:8837–8846. [PubMed: 23009666]

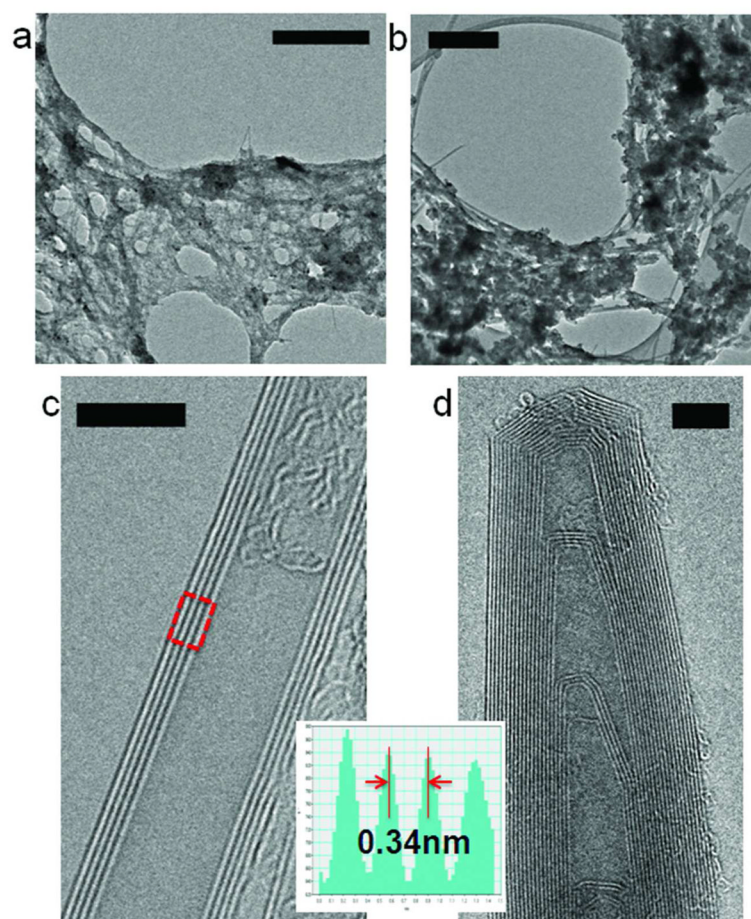


**Figure 1.** TEM images of as-synthesized carbon nanotubes investigated in this study. (a) and (b) are low-magnification images of the chemical vapor deposition (a) and arc-discharge (b) grown carbon nanotube bundles. (c) and (d) are representative higher-magnification images of individual nanotubes found in (a) and (b), respectively. The line profile of the boxed area in (c) is inset, showing the 0.34 nm spacing between the graphitic walls. Scale bars in (a) and (b) represent 500 nm. Scale bars in (c) and (d) represent 5 nm.



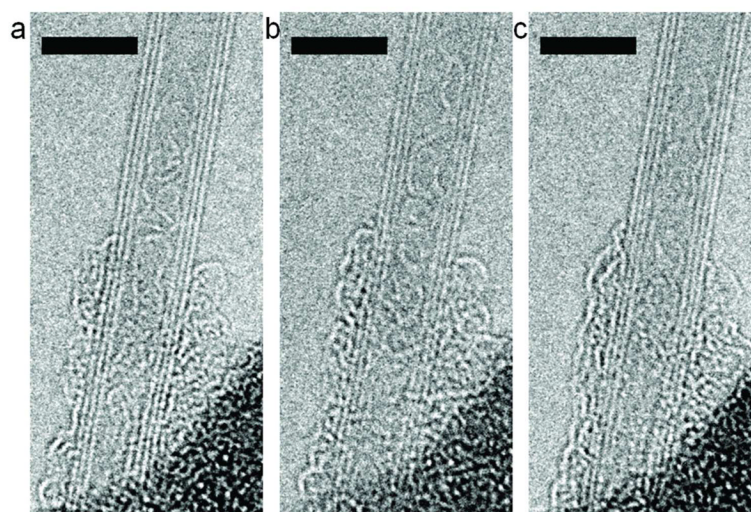


**Figure 2.** Aberration-corrected TEM images showing the same three-walled carbon nanotube during heating under high vacuum conditions. The images were taken at (a) 300°C, (b) 400°C and (c) 520°C. Scale bars equal 5 nm.

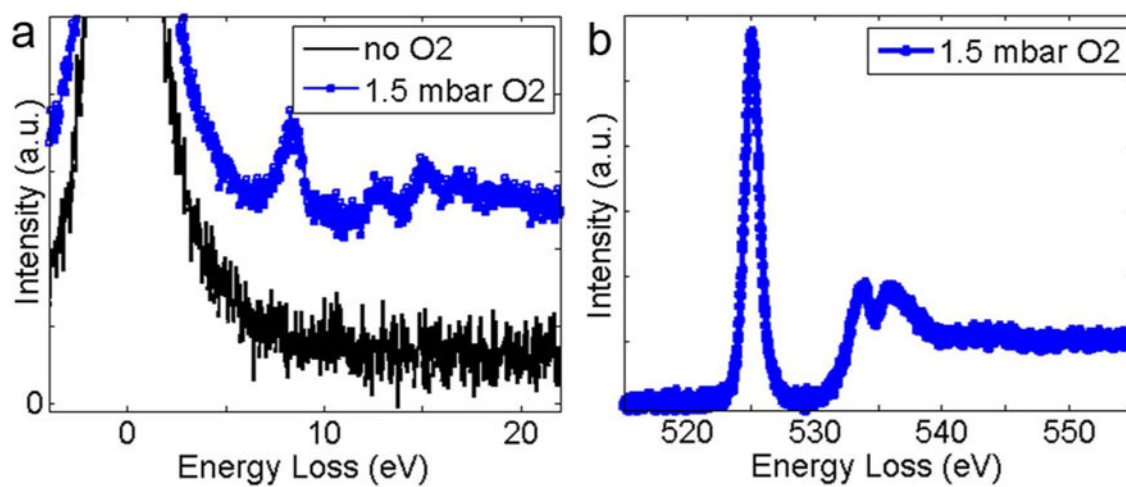


**Figure 3.**

EEL spectra show the presence of oxygen during the ETEM experiment. Low-energy oxygen peaks in (a) (blue spectrum) and the K-shell ionization peak for oxygen in (b) arise when the electron beam ionizes the oxygen gas.

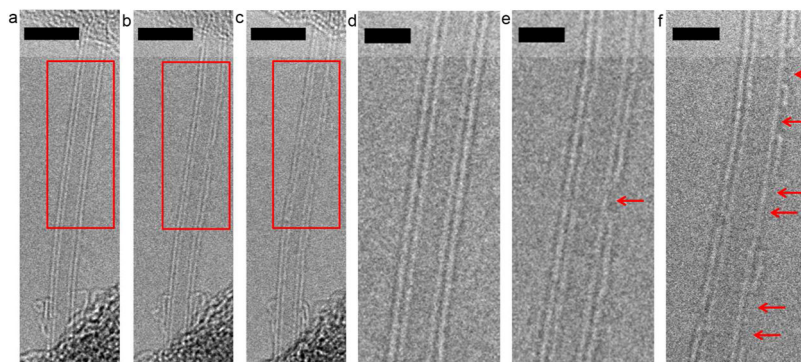


**Figure 4.** Aberration-corrected TEM images showing the structural changes in a double-walled carbon nanotube after being exposed to a heated, oxygen environment. These images show the same nanotube at 300°C before oxidation (a), at 300°C after 15 min exposure to 1.5 mbar oxygen (b), and at 400°C after 15 min exposure to 1.5 mbar oxygen (c). (d) to (f) are higher-magnification TEM images of insets (a) to (c) indicated by the red boxes. The outer wall of the nanotube (d) was successively etched away after exposure to oxygen at 300°C (e) and 400°C (f). Scale bars in (a) to (c) and (d) to (f) represent 5 nm and 2 nm, respectively.

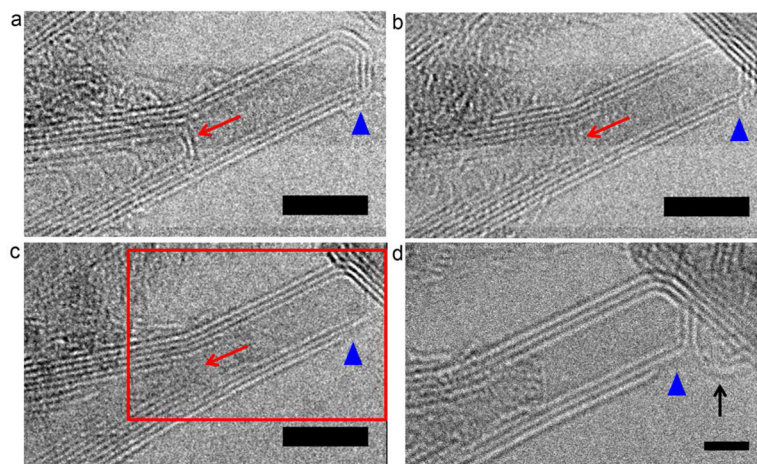


**Figure 5.** Observations at the ending cap of a CNT during oxidation. The inner walls and outer wall of the nanotube at 300°C (a) were removed after 1.5 mbar oxidation for 15 min at 300°C (red arrow and blue triangle) (b). More etching was observed after the same nanotube was oxidized for 15 min with 1.5 mbar oxygen at 400°C (c). The inset of (c) is shown in (d), where one can see the outermost wall being removed and dangling (black arrow) after oxidation at 400°C. Scale bars in (a) to (c) and (d) represent 5 nm and 2 nm, respectively.

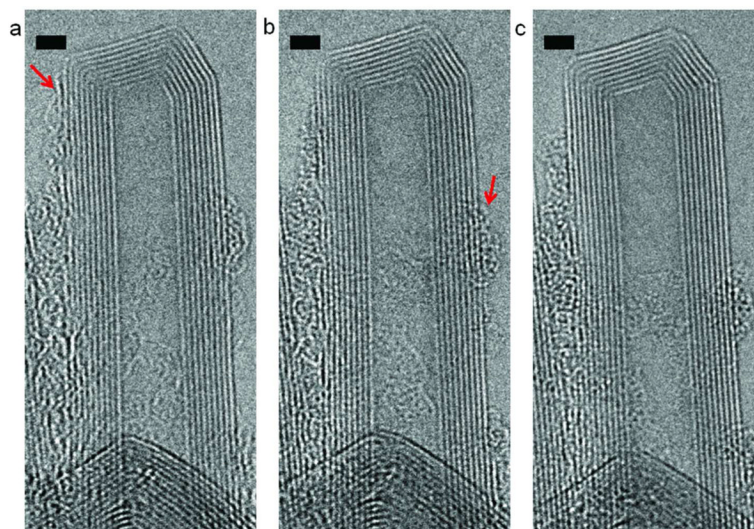


**Figure 6.** Carbon nanotubes with a greater number of graphitic layers are more resistant to oxidation. (a), (b) and (c) show images of the same nine-walled nanotube at 400°C, 400°C after 1.5 mbar oxidation and 520°C after 1.5 mbar oxidation, respectively. All walls of the nanotube remain intact after oxidation. Part of the amorphous carbon layer surrounding the nanotube (red arrows) appears to have been removed.

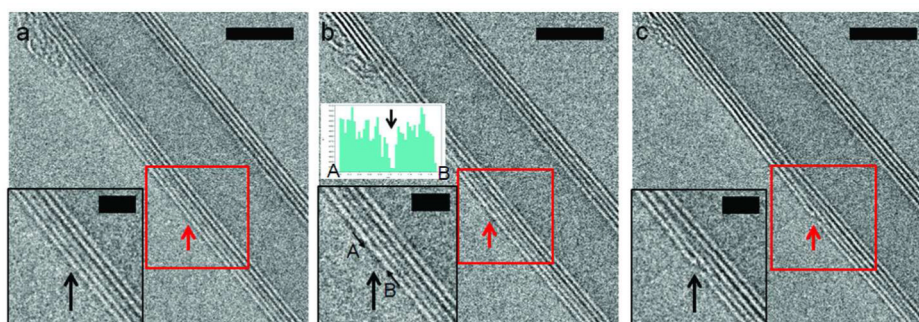


**Figure 7.** Observations of a possible initiation site for outer wall oxidation. (a), (b) and (c) are images of the same nanotube at 400°C, 400°C after 1.5 mbar oxidation and 520°C after 1.5 mbar oxidation, respectively. The red arrow in (b) shows a darker image spot which appears to be the initiation site for oxidation (red arrow in (c)). The insets are higher magnification images of the areas indicated by the red boxes. The line profile taken along A–B (inset of (b)) is shown above its inset, where the arrow corresponds to the darker image spot. Scale bars in (a) to (c) represent 5 nm. Scale bars in the insets represent 2 nm.